

# Direct Spectroscopic Observation of Fe(III)–Phenolate Complex Formed From the Reaction of Benzene With Peroxide Species on Fe/ZSM-5 At Room Temperature

Haian Xia, Keqiang Sun,<sup>†</sup> Keju Sun, Zhaochi Feng, Wei Xue Li, and Can Li\*

State Key Laboratory of Catalysis, Dalian Institute of Chemical Physics, Chinese Academy of Sciences, 457 Zhongshan Road, Dalian 116023, China

Received: January 17, 2008; Revised Manuscript Received: March 20, 2008

The reaction of benzene with the active oxygen species was studied by UV–visible diffuse reflectance and Raman spectroscopies. For the first time, the intermediate Fe(III)–phenolate complex was evidenced by a UV–visible absorption band at 690 nm and the Raman bands at 643, 896, 990, 1149, 1228, 1475, 1580, and 1607  $\text{cm}^{-1}$ . The Raman bands of the Fe(III)–phenolate complex were also confirmed by density functional theory calculations.

## Introduction

Phenol is an important industrial feedstock that serves as a precursor for phenol resins, fibers, dyestuffs, and medicine. The direct oxidation of benzene to phenol is one of the most challenging reactions in the field of catalytic chemistry.<sup>1–5</sup> It was found that a special Fe–oxo species, which was formed after high temperature pretreatment of Fe/ZSM-5 followed by reaction with  $\text{N}_2\text{O}$ , could selectively oxidize methane and benzene even at 243 K, which mimics the biocatalysis of soluble methane monooxygenase (sMMO).<sup>4</sup> It was found that the active oxygen species generated on Fe/ZSM-5 can oxidize benzene to phenol in a one-step method at high temperature.<sup>1–7</sup> These findings have received much attention in studying the active oxygen species as well as the reaction intermediate for the selective oxidation of benzene, particularly the reaction intermediate involved in the mechanism.

Great attempts have been undertaken to study the reaction of benzene with the active oxygen species on Fe/ZSM-5; however, the active sites and the reaction mechanism are still under debate. The isolated iron sites,<sup>1–3,8–11</sup> and binuclear iron sites<sup>5,11,12</sup> have been proposed to be active sites for benzene to phenol with  $\text{N}_2\text{O}$  as an oxidant. On the basis of theoretical calculations, van Santen and co-workers proposed that the reaction of benzene with the active oxygen species bound to isolated iron sites forms arene oxides, which is converted to an intermediate-adsorbed keto tautomer of phenol.<sup>10</sup> Ryder et al. proposed that the peroxide bound to isolated active centers ( $\text{Z}^-[\text{FeO}_2]^+$ ) are responsible for benzene oxidation via insertion of oxygen into the C–H bond of benzene based on theoretical calculations.<sup>9</sup> Yoshizawa and co-workers assumed that the conversion of benzene to phenol by  $\text{FeO}^+$  species is through a concerted reaction pathway, via neither radical species nor ionic intermediates. These authors proposed that the reaction is initiated by C–H activation of benzene, and takes place through the formation of the hydroxyl intermediate,  $\text{OH}-\text{Fe}^+-\text{C}_6\text{H}_5$ , which then transforms into  $\text{Fe}^+(\text{C}_6\text{H}_5\text{OH})$ , followed by a dissociation into phenol and  $\text{Fe}^+$ .<sup>8,13</sup> Dubkov et al. proposed that the oxidation of benzene by  $\alpha$ -oxygen species bound to a

binuclear Fe sites proceeds through the initial formation of unstable arene oxides, which can spontaneously isomerize into a phenolic product, based on kinetic and IR results.<sup>14,15</sup> Unfortunately, there is only limited experimental evidence on the nature of the active oxygen and the reaction intermediate involved in the selective oxidation of benzene. Therefore, it is still a challenge to experimentally characterize the active oxygen species and reaction intermediates in order to understand the mechanism of the selective oxidation of benzene in Fe/ZSM-5 systems.

We have demonstrated that UV resonance Raman spectroscopy can successfully identify transition metal atoms incorporated in zeolites, such as framework Fe ions in Fe/ZSM-5 and framework Ti ions in TS-1 zeolites.<sup>16,17</sup> In this work, we present a Raman spectroscopic identification of the reaction intermediate formed from the reaction of benzene with the active oxygen species in Fe/ZSM-5. For the first time, the Fe(III)–phenolate intermediate formed from the reaction of benzene with the active oxygen species on Fe/ZSM-5 at room temperature was detected by UV–visible and Raman spectroscopies, and this result was further confirmed by density functional theory (DFT) calculations.

## Experimental Section

The catalyst was synthesized by the solid-state ion-exchange method, the details have been given elsewhere.<sup>18,19</sup> The sample calcined in  $\text{O}_2$  atmosphere at 823 K was then treated in He atmosphere at 1173 K for 2 h. The iron content of the catalyst is about 2.2 wt.% analyzed by inductively coupled plasma (ICP) analyzer, corresponding to  $\text{Fe}/\text{Al} = 0.61$ . X-ray diffraction (XRD) measurements show that the MFI structure of the zeolite is not destroyed after high-temperature treatment.

Two methods were applied to determine the concentration of the Fe(II) sites. The first one is similar to the transient-response technique adopted by Kiwi-Minisker and co-workers.<sup>20</sup> The reaction effluent is continuously monitored by a calibrated online mass spectrometer (Gam 200, Pfeiffer Vacuum) after a step change from He flow to 5.0 vol %  $\text{N}_2\text{O}/\text{He}$  flow. Quantification of the amount of  $\text{N}_2$  evolved is used to determine the concentration of the Fe(II) sites based on the assumption that one oxygen atom is deposited per Fe(II) site.<sup>12,20</sup> Typically, 50 mg catalyst sample was used to determine the concentration of the Fe(II) sites in the Fe/ZSM-5 catalyst. Prior to each run, the catalyst was treated in He at 1173 K for 2 h and then cooled

\* To whom correspondence should be addressed. Tel: 86-411-84379070. Fax: +86-411-84694447. E-mail: canli@dicp.ac.cn.

<sup>†</sup> Present address: Innovative Catalysis Program, Key Lab of Organic Optoelectronics & Molecular Engineering, Department of Chemistry, Tsinghua University, Beijing 100084, China.

to 523 K in He. Subsequently, the concentration of N<sub>2</sub>O was quickly changed from 0 to 5.0 vol % N<sub>2</sub>O. A complementary method was used to determine the amount of deposited oxygen species via their reaction with methane at 373 K. It was assumed that one methane molecule reacts with two atomic oxygen species to form adsorbed methoxy and hydroxyl groups.<sup>4,18</sup>

The reaction effluent of benzene with the active oxygen species is monitored by an online mass spectrometer (Gam 200, Pfeiffer Vacuum). The following peaks were detected simultaneously: 4 (He), 18 (H<sub>2</sub>O), 28 (N<sub>2</sub>, CO), 32 (O<sub>2</sub>), 44 (CO<sub>2</sub>, N<sub>2</sub>O), 78 (C<sub>6</sub>H<sub>6</sub>), and 94 (C<sub>6</sub>H<sub>6</sub>O). The experimental steps are described as follows: first, forming the active oxygen species by introducing 5.0 vol % N<sub>2</sub>O to the catalyst at 523 K; then, cooling to room temperature, followed by pulsing 1 μL benzene to the catalyst in He flow via a special injector; after the reaction, switching to 0.5 vol % H<sub>2</sub>O/Ar and then ramping the temperature to 773 K; finally, cooling to 473 K and purging in He flow, and then temperature-programmed desorption in He flow.

UV–visible diffuse reflectance spectra (DRS) were recorded on a JASCO V-550 UV–visible spectrophotometer with an integrating sphere coated with BaSO<sub>4</sub>. The sample powder was loaded in a quartz cell. The details of the treatment processes are described as follows: treating the sample at 823 K in a flow of O<sub>2</sub> for 1 h to remove organic remnants, followed by a pretreatment in flowing He at 1173 K for 1 h; then, introducing 5 vol % N<sub>2</sub>O to the catalyst at 523 K; finally, exposing the catalyst to benzene at room temperature. For comparison, the catalyst was pretreated in He flow at 1173 K for 1 h, and then was exposed to benzene at room temperature. After each treatment, the quartz cell was quickly sealed and cooled to room temperature for recording UV–visible diffuse reflectance spectrum.

Visible Raman spectra were collected on a Spex 1877D Raman spectrograph with a laser line at 605 nm. The sample was pressed into a thin disk and fixed in a quartz cell. The same sequence of experimental steps as in the UV–visible experiments was used.

DFT calculations were performed using the Gaussian 03 program.<sup>21</sup> The B3LYP functional was employed. A 6-31 G\* basis set was used for all types of atoms. A binuclear Fe model was proposed according to the literature.<sup>22–26</sup> A dehydroxylated binuclear Fe(II) site is proposed to be the active site as a model for calculations, as high temperature treatment leads to the self-reduction and dehydroxylation of Fe(III) sites.<sup>12,24,27</sup> The zeolite framework is represented by a cluster composed of a pair of 5T rings sharing an edge. The binuclear Fe sites are bound to the Al sites located in T9 and T12 sites through extra-framework oxygen atoms. The Si–O bonds not belonging to the 5T rings were replaced by terminal Si–H bonds oriented in the direction of the former Si–O bonds.

## Results and Discussion

The concentration of the active sites on Fe/ZSM-5 was estimated by N<sub>2</sub>O decomposition at 523 K, i.e., via the reaction Fe–( ) + N<sub>2</sub>O → N<sub>2</sub> + Fe–(O).<sup>11,20</sup> Figure 1 shows the response of a step change from He flow to 5.0 vol % N<sub>2</sub>O/He flow on the Fe/ZSM-5 catalyst pretreated at 1173 K in He. A peak of N<sub>2</sub> was observed only, and no O<sub>2</sub> was detected in the effluent, suggesting that the Fe–oxo species was formed on Fe/ZSM-5.<sup>11,20</sup> The concentration of the deposited oxygen species estimated from the amount of the released N<sub>2</sub> is about 1.1 × 10<sup>−4</sup> mol/g, corresponding to an O/Fe ratio of 0.28. The amount of the deposited oxygen was further quantified by an immediately successive pulse of a known amount of methane to Fe/ZSM-5

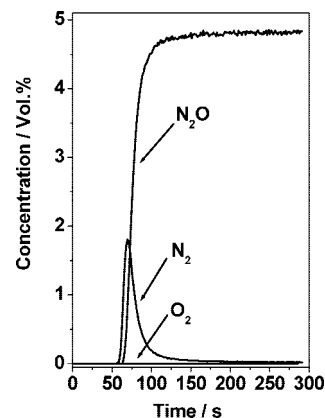


**Figure 1.** Response of a step from He flow to 5.0 vol % N<sub>2</sub>O/He flow at 523 K on the Fe/ZSM-5 catalyst pretreated at 1173 K in He.

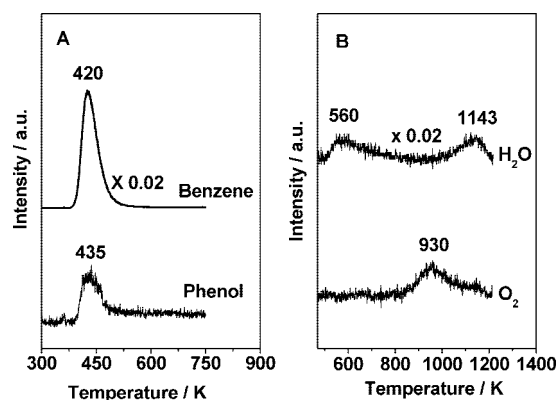


**Figure 2.** (A) Programmed-temperature desorption in 0.5 vol % H<sub>2</sub>O/He flow after the reaction of benzene with the active oxygen species at room temperature, followed by (B) programmed-temperature desorption in He flow after cooling to 473 K and purging in He flow.

at 373 K (not shown). The amount of surface oxygen species active for methane is about 9.3 × 10<sup>−5</sup> mol/g, corresponding to an O/Fe ratio of 0.24. This suggests that only a portion of the iron sites could form the active oxygen species reactive toward methane.

It has been reported that the reaction of the active oxygen species with benzene at room temperature is a stoichiometric reaction because the reaction intermediate is strongly adsorbed on the iron sites, and the phenol product was obtained by hydrolysis with solution of methanol and water.<sup>4</sup> Thus, the hydrolysis process was performed by introducing 0.5 vol % H<sub>2</sub>O/He to the catalyst after the reaction of the active oxygen species with benzene at room temperature (Figure 2A). As can be seen in Figure 2A, a desorption peak of phenol is observed, suggesting that the reaction intermediate can convert to phenol after hydrolysis. After the hydrolysis, the catalyst was cooled to 473 K and purged in He flow, and then a programmed-temperature desorption in He flow was performed (Figure 2B). The desorption peaks of O<sub>2</sub> and H<sub>2</sub>O are observed, indicating that high temperature treatment leads to the self-reduction of the iron sites.

Figure 3a shows the UV–visible diffuse reflectance spectrum of the catalyst pretreated at 1173 K in He flow. Two bands at 260 and 340 nm and a shoulder at 480 nm are observed. The bands at 260 and 340 nm are assigned to oxygen-to-iron charge transfer transition of isolated Fe ions and oligo-nuclear Fe clusters, respectively, and the band at 480 nm is associated with small iron oxide particles.<sup>19</sup> Figure 3b shows that a new band with a maximum around 605 nm is observed after exposing

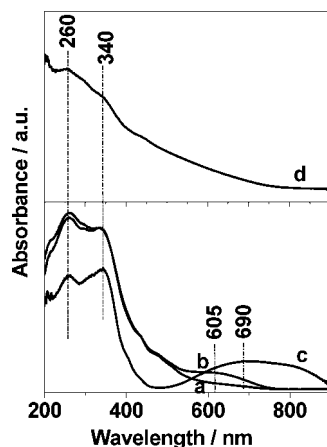


**Figure 3.** UV–visible diffuse reflectance spectra of Fe/ZSM-5 (a) after pretreatment at 1173 K in He flow, (b) after exposing the high-temperature pretreated Fe/ZSM-5 to  $N_2O$  at 523 K, (c) after the reaction of benzene with the Fe/ZSM-5 preloaded with the active oxygen species at room temperature, and (d) after benzene adsorbed on the Fe/ZSM-5 without the preloaded active oxygen species at room temperature.

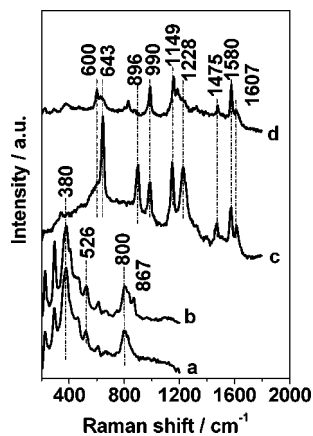


**Figure 4.** (A) Visible Raman spectra of Fe/ZSM-5 (a) after pretreatment at 1173 K in He flow, (b) after exposing the high-temperature-pretreated Fe/ZSM-5 to  $N_2O$  at 523 K, (c) after the reaction of benzene with the Fe/ZSM-5 preloaded with the active oxygen species at room temperature, and (d) after benzene adsorbed on the Fe/ZSM-5 without the preloaded active oxygen at room temperature. The excitation line: 605 nm.

the high-temperature pretreated Fe/ZSM-5 to  $N_2O$  at 523 K. A band at 340 nm together with a broadband in 500–900 nm centered at 690 nm appears after a subsequent exposure of the oxygen-containing sample to benzene at room temperature (Figure 3c). Accordingly, the color of the sample changes from white to blue along with the reaction. For comparison, the blank experiment of benzene adsorption on Fe/ZSM-5 without the preloaded active oxygen species gives rise to two bands at 260 and 340 nm (Figure 3d), which are associated with the isolated iron sites and oligo-nuclear iron clusters, respectively.

Figure 4a shows the visible Raman spectrum of the Fe/ZSM-5 after pretreatment in He at 1173 K with the excitation line at 605 nm, which just falls in the electronic band of the active oxygen species (Figure 3b). Raman bands at 380, 526, and 800  $cm^{-1}$  are observed. The bands at 380 and 800  $cm^{-1}$  are due to the MFI structure of ZSM-5,<sup>17</sup> and the band at 526  $cm^{-1}$  is tentatively assigned to Fe–O–Si symmetric vibrational mode of the oligo-nuclear Fe clusters.<sup>17</sup> Figure 4b shows the spectrum collected after exposing the high-temperature-pretreated Fe/ZSM-5 to  $N_2O$  at 523 K. It is worth noting that a new band at 867  $cm^{-1}$  appears after the reaction. After the reaction of

**TABLE 1: The Raman Bands of the Active Oxygen Species and the Fe(III)–Phenolate Complex Formed from the Reaction of Benzene with the Active Oxygen Species on Fe/ZSM-5 at Room Temperature**

experimental ( $cm^{-1}$ )	DFT ( $cm^{-1}$ )	assignment
643	645	$\nu(Fe-O)$
867	823	$\nu(O-O)$
896	881	$\nu(Fe-O) + \nu(C=C)$
990	1010	phenyl ring breath
1149	1105	$\nu(C-H)$
1228	1254	$\nu(C-O)$
1475	1480	$\nu(C=C)$
1580	1619	$\nu(C=C)$
1607	1630	$\nu(C=C)$

benzene with Fe/ZSM-5 preloaded with the active oxygen species (Figure 4c), a number of evident Raman bands are observed at 643, 896, 990, 1149, 1228, 1475, 1580, and 1607  $cm^{-1}$ . Figure 4d shows the Raman spectrum of benzene adsorbed on Fe/ZSM-5 without the preloaded active oxygen species. Raman bands are observed at 600, 990, 1149, 1475, 1580, and 1607  $cm^{-1}$  and are mainly due to adsorbed benzene on Fe/ZSM-5. Compared with spectrum recorded after the reaction of benzene with Fe/ZSM-5 preloaded with the reactive oxygen species (Figure 4c), the three characteristic Raman bands at 643, 896, and 1228  $cm^{-1}$  were missing (Figure 4d), indicating the three new bands are associated with the species different from the adsorbed benzene.

The previous characterization of iron–oxo complexes in inorganic chemistry and in biological sMMO has revealed that dinuclear Fe–peroxo species normally exhibit electronic absorptions in the 570–750 nm region due to peroxo-to-iron charge-transfer bands, and show the  $\nu_{O-O}$  frequency in the 850–900  $cm^{-1}$  region.<sup>28,29</sup> For Fe/ZSM-5, the Raman band at 867  $cm^{-1}$  and the absorption band around 605 nm fall just within the 850–890  $cm^{-1}$  and 570–750 nm regions because of the peroxide ions bridged on the binuclear iron sites in sMMO and its model compounds, respectively. Therefore, the active oxygen species could be a peroxo species bridged on a dinuclear iron site. The assignment of the characteristic Raman band at 867  $cm^{-1}$  to the peroxide bridged on a binuclear Fe sites is also supported by the DFT calculations result reported recently by Yang et al.<sup>30</sup>

It was reported that Fe(III)–phenolate complexes<sup>31,32</sup> and the decay product of peroxo species in ribonucleotide reductase<sup>33</sup> exhibit the absorption bands in the 600–900 nm region, which have been assigned to the phenolate-to-Fe(III) charge transfer transition. The Raman spectra of Fe(III)–phenolate complexes are dominated by a set of phenolate vibrational modes at 615, 630, 895, 1120, 1280, 1330, 1450, 1475, 1560, and 1600  $cm^{-1}$  and electric absorption bands in the 440–690 nm region.<sup>31,32</sup> Comparing the spectral features of the reaction intermediate formed from benzene reaction with the active oxygen species in Fe/ZSM-5 with those of enzymes and Fe(III)–phenolate complexes, we can easily find remarkable similarities between them. Thus, the absorption band around 690 nm can be assigned to the charge transfer transition from phenolate to Fe(III), and the Raman bands at 643, 896, 990, 1149, 1228, 1475, 1580, and 1607  $cm^{-1}$  are attributed to an Fe(III)–phenolate complex. For example, the Raman bands at 643 and 1228  $cm^{-1}$  are ascribed to  $\nu(Fe-O)$  and  $\nu(C-O)$  modes,<sup>31,32</sup> respectively.

To clarify the assignments described above, DFT calculations were performed. The calculated vibrational frequencies and corresponding modes of the reaction intermediate are listed in

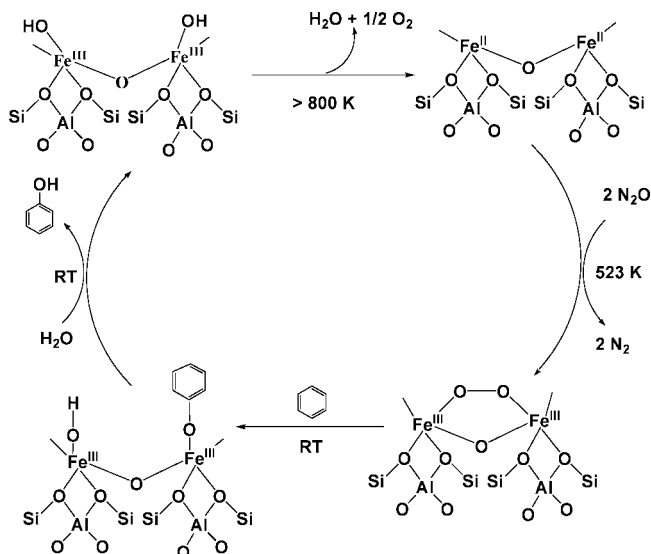


**Figure 5.** Schematic description of the reaction pathway of the active oxygen species with benzene on Fe/ZSM-5 at room temperature.

Table 1. The calculated results are close to the experimental results. The  $\nu(\text{O}-\text{O})$  mode calculated for peroxo species bridged on the binuclear Fe sites is about  $823\text{ cm}^{-1}$ , which is close to experimental result of  $867\text{ cm}^{-1}$ . A band at  $645\text{ cm}^{-1}$  is ascribed to a  $\nu(\text{Fe}-\text{O})$  mode, and a band at  $1254\text{ cm}^{-1}$  is assigned to a  $\nu(\text{C}-\text{O})$  mode. Therefore, it is clear that the Raman bands at  $643, 896, 990, 1149, 1228, 1475, 1580,$  and  $1607\text{ cm}^{-1}$  are due to the Fe(III)–phenolate complex, an intermediate formed from the reaction of benzene and the active oxygen species at room temperature.

The Raman spectral results clearly demonstrate that the peroxide bridged on the binuclear iron sites directly react with benzene to form an Fe(III)–phenolate intermediate. The Fe(III)–phenolate complex bound to the binuclear iron sites could transform into the hydroxylated binuclear iron sites by releasing phenol molecules after hydrolysis (Figure 2A), which is similar to the hydrolysis of methoxy species bound at the iron sites.<sup>4,34</sup> The hydroxylated binuclear iron sites could convert into the dehydroxylated binuclear iron sites by releasing  $\text{H}_2\text{O}$  and  $\text{O}_2$  upon high temperature treatment (Figure 2B), which is also confirmed by the results.<sup>24,26,35</sup> To schematically describe the reaction of the active oxygen species with benzene on Fe/ZSM-5 at room temperature, a possible reaction pathway is shown in Figure 5.

It should be pointed out that the reaction of benzene with the active oxygen species at room temperature is a stoichiometric reaction, which might be different from the benzene-to-phenol steady-state catalytic oxidation at high temperatures ( $>573\text{ K}$ ). So, the Fe(III)–phenolate intermediate could be one of the precursors of phenol product or byproducts (e.g.,  $\text{CO}_2$ , deposited coke, etc.) under catalytic reaction conditions.

## Conclusions

A UV–visible absorption band at  $605\text{ nm}$  and Raman band at  $867\text{ cm}^{-1}$  are observed after the  $\text{N}_2\text{O}$  decomposition at  $523\text{ K}$  on the Fe/ZSM-5 pretreated in He at  $1173\text{ K}$ , which could be assigned to a peroxide bridged on the binuclear iron sites. It was found that an Fe(III)–phenolate intermediate is formed from the reaction of benzene with the active oxygen species at room temperature, characterized by the absorption band at  $690\text{ nm}$  and the Raman bands at  $643, 896, 990, 1149, 1228, 1475, 1580,$  and  $1607\text{ cm}^{-1}$ . The assignments of the Raman bands to the

Fe(III)–phenolate complex are also confirmed by DFT calculations. The Fe(III)–phenolate intermediate could be converted to phenol after hydrolysis.

**Acknowledgment.** This work was financially supported by the National Basic Research Program of China (2005CB221407) and the National Natural Science Foundation of China (Grant No. 20673115, 20773118).

## References and Notes

- Jia, J. F.; Pillai, K. S.; Sachtler, W. M. H. *J. Catal.* **2004**, *221*, 119.
- Hensen, E. J. M.; Zhu, Q.; Janssen, R. A. J.; Magusin, P.; Kooyman, P. J.; van Santen, R. A. *J. Catal.* **2005**, *233*, 123.
- Hensen, E. J. M.; Zhu, Q.; van Santen, R. A. *J. Catal.* **2005**, *233*, 136.
- Panov, G. I.; Uriarte, A. K.; Rodkin, M. A.; Sobolev, V. I. *Catal. Today* **1998**, *41*, 365.
- Chemyavsky, V. S.; Pirutko, L. V.; Uriarte, A. K.; Kharitonov, A. S.; Panov, G. I. *J. Catal.* **2007**, *245*, 466.
- Centi, G.; Genovese, C.; Giordano, G.; Katovic, A.; Perathoner, S. *Catal. Today* **2004**, *91–92*, 17.
- Hensen, E.; Zhu, Q. J.; Liu, P. H.; Chao, K. J.; van Santen, R. J. *J. Catal.* **2004**, *226*, 466.
- Yoshizawa, K.; Shiota, Y.; Yamabe, T. *J. Am. Chem. Soc.* **1999**, *121*, 147.
- Ryder, J. A.; Chakraborty, A. K.; Bell, A. T. *J. Catal.* **2003**, *220*, 84.
- Kachurovskaya, N. A.; Zhidomirov, G. M.; Hensen, E. J. M.; van Santen, R. A. *Catal. Lett.* **2003**, *86*, 25.
- Yuranov, I.; Bulushev, D. A.; Renken, A.; Kiwi-Minsker, L. J. *J. Catal.* **2004**, *227*, 138.
- Dubkov, K. A.; Ovanesyan, N. S.; Shteinman, A. A.; Starokon, E. V.; Panov, G. I. *J. Catal.* **2002**, *207*, 341.
- Yoshizawa, K.; Shiota, Y.; Yumura, T.; Yamabe, T. *J. Phys. Chem. B* **2000**, *104*, 734.
- Dubkov, K. A.; Sobolev, V. I.; Talsi, E. P.; Rodkin, M. A.; Watkins, N. H.; Shteinman, A. A.; Panov, G. I. *J. Mol. Catal. A* **1997**, *123*, 155.
- Panov, G. I.; Dubkov, K. A.; Paukshtis, Y. A. *Catalysis by Unique Metal Ion Structures in Solid Matrices*; Kluwer Academic: Dordrecht, The Netherlands/Norwell, MA, 2001.
- Li, C.; Xiong, G.; Xin, Q.; Liu, J. K.; Ying, P. L.; Feng, Z. C.; Li, J.; Yang, W. B.; Wang, Y. Z.; Wang, G. R.; Liu, X. Y.; Lin, M.; Wang, X. Q.; Min, E. Z. *Angew. Chem. Int. Ed.* **1999**, *38*, 2220.
- Li, C. *J. Catal.* **2003**, *216*, 203.
- Sun, K. Q.; Zhang, H. D.; Xia, H.; Lian, Y. X.; Li, Y.; Feng, Z. C.; Ying, P. L.; Li, C. *Chem. Commun.* **2004**, 2480.
- Sun, K. Q.; Xia, H.; Hensen, E.; van Santen, R.; Li, C. *J. Catal.* **2006**, *238*, 186.
- Kiwi-Minsker, L.; Bulushev, D. A.; Renken, A. *J. Catal.* **2003**, *219*, 273.
- Frisch, M. J.; Trucks, G. W.; Schlegel, H. B.; Scuseria, G. E.; Robb, M. A.; Cheeseman, J. R.; Montgomery, J. A., Jr.; Vreven, T.; Kudin, K. N.; Burant, J. C.; Millam, J. M.; Iyengar, S. S.; Tomasi, J.; Barone, V.; Mennucci, B.; Cossi, M.; Scalmani, G.; Rega, N.; Petersson, G. A.; Nakatsuji, H.; Hada, M.; Ehara, M.; Toyota, K.; Fukuda, R.; Hasegawa, J.; Ishida, M.; Nakajima, T.; Honda, Y.; Kitao, O.; Nakai, H.; Klene, M.; Li, X.; Knox, J. E.; Hratchian, H. P.; Cross, J. B.; Adamo, C.; Jaramillo, J.; Gomperts, R.; Stratmann, R. E.; Yazyev, O.; Austin, A. J.; Cammi, R.; Pomelli, C.; Ochterski, J. W.; Ayala, P. Y.; Morokuma, K.; Voth, G. A.; Salvador, P.; Dannenberg, J. J.; Zakrzewski, V. G.; Dapprich, S.; Daniels, A. D.; Strain, M. C.; Farkas, O.; Malick, D. K.; Rabuck, A. D.; Raghavachari, K.; Foresman, J. B.; Ortiz, J. V.; Cui, Q.; Baboul, A. G.; Clifford, S.; Cioslowski, J.; Stefanov, B. B.; Liu, G.; Liashenko, A.; Piskorz, P.; Komaromi, I.; Martin, R. L.; Fox, D. J.; Keith, T.; Al-Laham, M. A.; Peng, C. Y.; Nanayakkara, A.; Challacombe, M.; Gill, P. M. W.; Johnson, B.; Chen, W.; Wong, M. W.; Gonzalez, C.; Pople, J. A. *Gaussian 03*; Gaussian, Inc.: Pittsburgh, PA, 2003.
- Chen, H. Y.; Sachtler, W. M. H. *Catal. Today* **1998**, *42*, 73.
- Marturano, P.; Drozdova, L.; Kogelbauer, A.; Prins, R. *J. Catal.* **2000**, *192*, 236.
- El-Malki, E. M.; van Santen, R. A.; Sachtler, W. M. H. *J. Catal.* **2000**, *196*, 212.
- Yakovlev, A. L.; Zhidomirov, G. M.; van Santen, R. A. *J. Phys. Chem. B* **2001**, *105*, 12297.
- Hansen, N.; Heyden, A.; Bell, A. T.; Keil, F. J. *J. Catal.* **2007**, *248*, 213.
- Pirngruber, G. D.; Roy, P. K.; Prins, R. *J. Catal.* **2007**, *246*, 147.

(28) Brunold, T. C.; Tamura, N.; Kitajima, N.; Moro-oka, Y.; Solomon, E. I. *J. Am. Chem. Soc.* **1998**, *120*, 5674.

(29) Girerd, J. J.; Banse, F.; Simaan, A. J. *Metal-Oxo and Metal-Peroxo Species in Catalytic Oxidation, Structure and Bonding*; Springer: Berlin, 2000.

(30) Yang, G.; Zhou, L. J.; Liu, X. C.; Han, X. W.; Bao, X. H. *Catal. Commun.* **2007**, *8*, 1981.

(31) Carrano, C. J.; Carrano, M. W.; Sharma, K.; Backes, G.; Sanders-Loehr, J. *Inorg. Chem.* **1990**, *29*, 1865.

(32) Jensen, M. P.; Lange, S. J.; Mehn, M. P.; Que, E. L.; Que, L. *J. Am. Chem. Soc.* **2003**, *125*, 2113.

(33) Baldwin, J.; Voegtli, W. C.; Khidekel, N.; Moenne-Loccoz, P.; Krebs, C.; Pereira, A. S.; Ley, B. A.; Huynh, B. H.; Loehr, T. M.; Riggs-Gelasco, P. J.; Rosenzweig, A. C.; Bollinger, J. M. *J. Am. Chem. Soc.* **2001**, *123*, 7017.

(34) Wood, B. R.; Reimer, J. A.; Bell, A. T.; Janicke, M. T.; Ott, K. C. *J. Catal.* **2004**, *225*, 300.

(35) Battiston, A. A.; Bitter, J. H.; de Groot, F. M. F.; Overweg, A. R.; Stephan, O.; van Bokhoven, J. A.; Kooyman, P. J.; van der Spek, C.; Vanko, G.; Koningsberger, D. C. *J. Catal.* **2003**, *213*, 251.

JP800455X